AlGaAs Ambient Light Detectors With a Human-Eye Spectral Response

Tzu-Chiang Lin, Ta-Chun Ma, and Hao-Hsiung Lin, *Senior Member, IEEE*

***Abstract*—We report an AlGaAs ambient light detector with a spectral response matched to Commission Internationale de l'Eclairage (CIE) photopic luminosity function. The detector consists of an $Al_{0.6}Ga_{0.4}As$ PIN junction for main absorption, a two-step-four-section compositional grading structure centered in the junction for auxiliary absorption, and a built-in filtering structure on top of the PIN junction. The peak responsivity of the detector is 0.096 A/W at 558 nm, which corresponds to 164 pA/lux in photometric unit. The CIE defined spectral mismatch index f_1' of the detector is as low as 5.8%.**

***Index Terms*—AlGaAs, ambient light detector, Commission Internationale de l'Eclairage (CIE) photopic luminosity function.**

I. Introduction

RECENTLY, ambient light detectors have drawn more and more attention due to the rapid growth of portable equipment such as personal digital assistants, notebooks, and mobile phones. Since the display backlighting of these types of portable equipment heavily drains current from the batteries, high-performance detectors are demanded to provide accurate measurement on ambient light condition for the brightness control so as to save power consumption and reduce users' eye strain. To achieve the optimum brightness, saving power without sacrificing display quality, the spectral response of ambient light detectors should be very close to that of human eyes. The Commission Internationale de l'Eclairage (CIE) has established two standard luminosity functions, scotopic and photopic functions, to represent the average sensitivity of human eyes [1]. The former is for a low illuminance level, while the latter is for ordinary illuminance level and best fits the human eyes in most conditions. Today, ambient light detectors are dominated by Si-based devices which are difficult in accurately matching to CIE photopic luminosity function. Due to the small energy gap, the spectral responses of Si detectors mostly extend to the invisible infrared (IR) range, resulting in significant mismatch to human eyes when the light sources, such as incandescent lamps or solar light, also emit IR lights. Solutions currently proposed to this problem include special structures to probe photons absorbed in specified depth [2]–[4], additional filter on detectors [5], and signal processing on the signals from two or three photodiodes with different spectral responses [6]. However, these solutions need either a complicated process or an extra circuit to obtain acceptable signals. In this letter, we propose a simpler approach based on AlGaAs ternary alloy to match CIE photopic luminosity function. In fact, AlGaAs is a well-studied and technologically mature semiconductor alloy. Its Γ bandgap covers a wide range from 1.42 to 2.95 eV [7], and can be tailored directly to the visible range required by the CIE function without the aforementioned complicated structures or circuits proposed for Si detectors. Moreover, the variety in the AlGaAs energy gap also allows the energy gap engineering for built-in filtering and absorption layers to embellish the spectral response. We demonstrate the design and fabrication of AlGaAs ambient light detector which is well-matched to CIE photopic luminosity function, needs no complex circuit, and can be produced by a very simple process.

TABLE I
Structure of Sample A

Layer	Material	Thickness	Density
Contact	p^+ GaAs	30 nm	10^{18} cm^{-3}
Filtering	$p^+Al_{0.74}Ga_{0.26}As$	300 nm	10^{18} cm^{-3}
Filtering	p^+ GaAs	70 nm	10^{18} cm^{-3}
Main Absorp	$p^+Al_{0.60}Ga_{0.40}As$	100 nm	10^{18} cm^{-3}
Main Absorp	i $Al_{0.60}Ga_{0.40}As$	150 nm	undoped
Sec. Absorp	i $Al_zGa_{1-z}As$ (z: 0.60 $\rightarrow$ 0.48)	150 nm	undoped
Sec. Absorp	i $Al_zGa_{1-z}As$ (z: 0.48 $\rightarrow$ 0.36)	110 nm	undoped
Sec. Absorp	i $Al_zGa_{1-z}As$ (z: 0.36 $\rightarrow$ 0.48)	110 nm	undoped
Sec. Absorp	i $Al_zGa_{1-z}As$ (z: 0.48 $\rightarrow$ 0.60)	150 nm	undoped
Main Absorp	i $Al_{0.60}Ga_{0.40}As$	150 nm	undoped
Main Absorp	n^+ $Al_{0.60}Ga_{0.40}As$	100 nm	10^{18} cm^{-3}
Buffer	n^+ GaAs	200 nm	10^{18} cm^{-3}
Substrate	n^+ GaAs	350 μm	~10^{17} cm^{-3}

II. Device Structure

The layer structure of the ambient light detector is detailed in Table I. The detector, with the band diagram at zero bias voltage shown in Fig. 1, is composed of three regions, the filtering region (region I), the main absorption region (region II), and the secondary absorption region (region III). The main absorption region is an $Al_{0.6}Ga_{0.4}As$ p-i-n homo-junction and contributes the major response of the detector. Though the energy gap of

Manuscript received January 10, 2008; revised April 4, 2008. This work was supported by the National Science Council, R.O.C. and by ADDtek Corp., under Contract NSC-92-2622-E-002-039-CC3.

T.-C. Lin and T.-C. Ma are with the Graduate Institute of Electronics Engineering, National Taiwan University, Taipei 106, Taiwan, R.O.C.

H.-H. Lin is with the Graduate Institute of Electronics Engineering, National Taiwan University, Taipei 106, Taiwan, R.O.C. He is also with the Department of Electrical Engineering and the Graduate Institute of Photonics and Optoelectronics, National Taiwan University (e-mail: hhlin@ntu.edu.tw).

Color versions of one or more of the figures in this letter are available online at http://ieeexplore.ieee.org.

Digital Object Identifier 10.1109/LPT.2008.926849

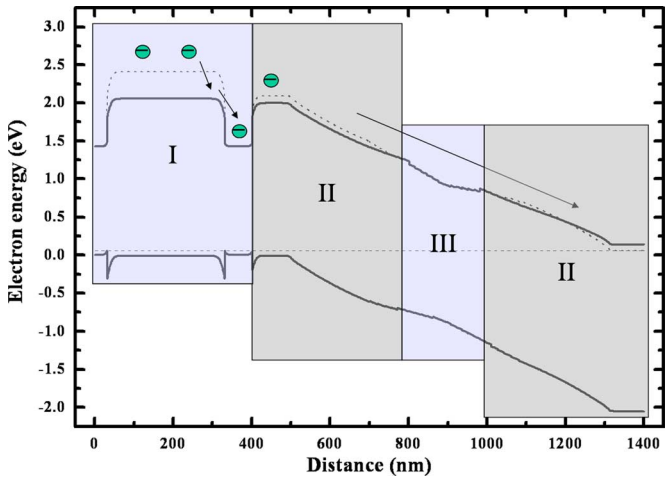

Fig. 1. Band diagram of the ambient light detector at zero bias voltage. Dotted line and solid line represent Γ-band and X-band, respectively. Marks I, II, and III indicate the filtering region, main absorption region, and secondary absorption region, respectively.

$Al_{0.6}Ga_{0.4}As$ is indirect, the cut-off wavelength of this junction is at ∼580 nm, indicating that the absorption mainly results from the direct Γ band. This cut-off wavelength is intentionally chosen to be slightly longer than the peak wavelength of CIE photopic luminosity function. Because the absorption edge of the $Al_{0.6}Ga_{0.4}As$ alloy is much sharper than the long wavelength shoulder of the CIE function, a compositional grading layer structure, i.e., the secondary absorption region, is used to embellish the long wavelength shoulder of the detector responsivity. Note that the energy gaps of the materials consisting of the region should be lower than that of the main absorption region. In order to avoid the formation of energy spikes or notches on the conduction and valence band edges, which may hinder the collection of the photogenerated carriers, the secondary absorption region is centered in the junction as can be seen in the band diagram shown in Fig. 1. The grading function of this region is composed of four grading sections which are mirror symmetric with respect to the center of the structure. The Al composition was first graded from 0.60 to 0.48 (the first section), and then from 0.48 to 0.36 (the second section). The third and fourth sections are the reverse of the second and first sections, respectively. Thickness and end compositions of each section were optimized by experiments. On top of the main absorption region, a GaAs–$Al_{0.74}Ga_{0.26}As$–GaAs triple-layer structure serves as the filtering region. The top 30-nm-thick GaAs is used to protect the high Al-containing $Al_{0.74}Ga_{0.26}As$ layer underneath it and to facilitate the formation of ohmic contact. The next $Al_{0.74}Ga_{0.26}As$ layer is designed to filter the short wavelength light below 530 nm so as to match the short wavelength side of CIE luminosity function. As can be seen in Fig. 1, the electrons generated from the absorbed photons in this layer will diffuse and be trapped in the two neighboring GaAs layers. Because of the low GaAs energy gap, the trapped electrons are not able to escape to the following junction. Instead, they are exhausted by recombining with the majority holes in the GaAs layers. In order to examine the filter ability of the GaAs–$Al_{0.74}Ga_{0.26}As$–GaAs structure, we have grown a series of samples, B, C, and D, with different AlGaAs thicknesses. Detailed structures are shown in Table II.

TABLE II
STRUCTURE OF SAMPLES B, C, AND D

Layer	Material	Thickness	Density
Contact	p^+ GaAs	30 nm	10^{18} cm^{-3}
Filtering	p^+ $Al_{0.73}Ga_{0.27}As$	1200 nm (B) 300 nm (C) 0 nm (D)	10^{18} cm^{-3}
Filtering	p^+ GaAs	70 nm	10^{18} cm^{-3}
Absorp	p^+ $Al_{0.57}Ga_{0.43}As$	200 nm	10^{18} cm^{-3}
Absorp	i $Al_{0.57}Ga_{0.43}As$	150 nm	undoped
Absorp	n^+ $Al_{0.57}Ga_{0.43}As$	200 nm	10^{18} cm^{-3}
Buffer	n^+ GaAs	200 nm	10^{18} cm^{-3}
Substrate	n^+ GaAs	350 μm	∼10^{17} cm^{-3}

III. EXPERIMENTAL PROCEDURES

All the samples in this study were grown on n^+-GaAs substrates by gas source molecular beam epitaxy. The Al beam and Ga beam were supplied by an Addon cold-lip K-cell and an EPI sumo-cell, respectively. The As_2 flux was supplied by a gas cell in which the AsH_3 precursor was cracked at 1000 °C. The beam flux was calibrated by an ion gauge. We used Si and Be as the n- and p-type impurities, respectively. The wafer was ramped to 600 °C and desorbed for 15 min to remove the oxides on the wafer surface. The structures listed in Tables I and II were then deposited on the substrates. The two-step-four-section grading layers were deposited by linearly increasing or decreasing the temperature of the Al K-cell.

To begin with the detector fabrication, the top electrode, Ti (20 nm)/Pt (20 nm)/Ti (20 nm)/Au (300 nm), was deposited and lifted-off on the p^+-GaAs contact layer by standard photolithography and e-beam evaporation. The bottom electrode, AuGeNi (150 nm)/Au (300 nm), was then deposited on the back side of the n^+-GaAs substrate. Finally, mesa etching was used to isolate the devices. The area of the detector is 1000×1000 μm^2. Spectral response measurement was performed using standard lock-in techniques and the device was under zero bias condition. The light source from an ASB-XE-175 Xe-lamp was first dispersed by a SPEX-500M spectrometer, and then was guided through an optical fiber bundle to a microscope where it was further focused on the devices. The light power was determined by using a calibrated Newport 818UV Si detector. Since the focused light spot is only 50 μm in diameter, much smaller than the sizes of the samples and the Newport 818 UV detector, we can ensure that both devices received equal light power in the measurement.

IV. RESULTS AND DISCUSSION

Fig. 2 shows the spectral response of samples B, C, and D. These three samples are with different $Al_{0.73}Ga_{0.27}As$ thickness: 1200, 300, and 0 nm. They are used to study the effect of $Al_{0.73}Ga_{0.27}As$ thickness on the performance of the triple-layer built-in filtering structure. For comparison, CIE photopic luminosity function is also depicted in Fig. 2. As can be seen in the short wavelength region, especially from 450 to 550 nm, the responsivity curve of sample C is parallel to that of the CIE

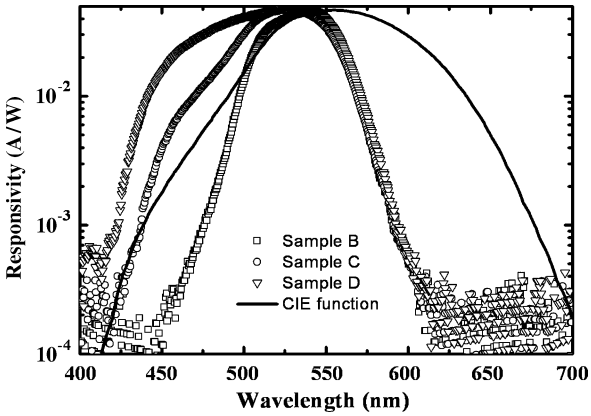

Fig. 2. Spectral responsivity of samples B, C, and D. CIE photopic luminosity function is also depicted in this plot for comparison.

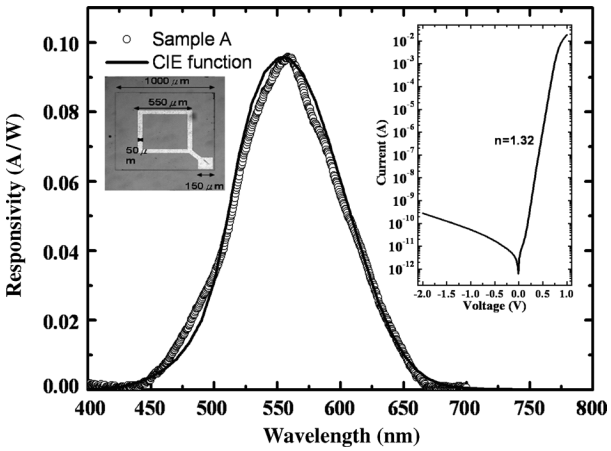

Fig. 3. Spectral responsivity of sample A. For comparison, CIE photopic luminosity function is also depicted. The right inset shows the I–V characteristics of the detector at room temperature. The left inset is a microscopic graph showing the detector.

function. Since the responsivity axis is in logarithm scale, it indicates that the structure of sample C can successfully match the CIE function. The slopes of samples B and D, however, are either too smooth or too sharp, and cannot meet the requirement of the CIE function. Therefore, the filtering structure of sample C is adopted. On the other hand, there is a large gap between the long wavelength shoulders of CIE photopic luminosity function and the samples. The shoulders of the three samples, which match together, are due to the absorption edge of the bottom $Al_{0.57}Ga_{0.43}As$ PIN junction. The aforementioned two-step-four-section grading structure is thus inserted into the center of the PIN junction to fill the gap. The spectral response of sample A, the final detector, is shown in Fig. 3. For comparison, CIE photopic luminosity function is also depicted. The peak wavelength and responsivity of the detector are 558 nm and 0.096 A/W, respectively. The responsivity amounts to an external quantum efficiency of 21%, which is limited by the surface reflection and the absorption by the GaAs layers of the filtering region and can be further improved by coating antireflection layers. In terms of photometric unit, the responsivity equals 164 pA/lux. The logarithm current–voltage (I–V) characteristic of the detector is shown in the inset of Fig. 3. The unpassivated junction shows a standard exponential behavior with a junction ideality factor of 1.32 over nine decades in its forward region and a dark current of 280 pA at −2-V reversed bias. To evaluate the mismatch between the detector and CIE photopic luminosity function, the CIE defined spectral mismatch index f_1' is used [8]. The index is given by

$$f_1' = \frac{\int |S_{\rm rel}^*(\lambda) - V(\lambda)|\, d\lambda}{\int V(\lambda) d\lambda} \tag{1}$$

where $V(\lambda)$ is CIE photopic luminosity function and $S_{\rm rel}^*$ is the normalized relative spectral response of sample A

$$S_{\rm rel}^*(\lambda) = \frac{\int S_A(\lambda) V(\lambda) d\lambda}{\int S_A(\lambda) S_{\rm rel}(\lambda) d\lambda} \cdot S_{\rm rel}(\lambda) \tag{2}$$

where $S_A(\lambda)$ is the spectral distribution data for CIE Illuminant A (2856 K Planckian radiation) [8], and $S_{\rm rel}(\lambda)$ is the measured responsivity of sample A. The mismatch index f_1' of sample A is only 5.8%, which outperforms most of the detectors [2]–[6].

V. Conclusion

We have successfully realized an AlGaAs ambient light detector highly matched to CIE photopic luminosity function. The device is with a built-in filtering structure and a two-step-four-section grading auxiliary absorption structure. The peak of the spectral responsivity is 0.096 A/W at 558 nm which amounts to 164 pA/lux. The CIE defined spectral mismatch index f_1' of the detector is 5.8%.

Acknowledgment

The authors would like to thank J.-Y. Wu, J.-P. Wang, and C.-H. Huang for their assistance in process and measurement development and J. Chiang of ADDtek Corp. for his valuable discussions.

References

[1] *Commission Internationale De L'Eclairage Proceedings*. Cambridge, U.K.: Cambridge Univ. Press, 1924, CIE.
[2] H.-K. Tsai, S.-C. Lee, and W.-L. Lin, "An amorphous SiC/Si two-color detector," *IEEE Electron Device Lett.*, vol. 8, no. 8, pp. 365–367, Aug. 1987.
[3] M. Topic, H. Stiebig, D. Knipp, and F. Smole, "Optimization of a-Si:H-based three-terminal three-color detectors," *IEEE Trans. Electron Devices*, vol. 46, no. 9, pp. 1839–1845, Sep. 1999.
[4] M. Chouikha, F. Vienot, and G. N. Lu, "Colorimetric characterization of a buried triple p-n junction photodetector," *Displays*, vol. 19, pp. 105–110, 1998.
[5] R. F. Wolffenbuttel, "Color filters integrated with the detector in silicon," *IEEE Electron Device Lett.*, vol. EDL-8, no. 1, pp. 13–15, Jan. 1987.
[6] H.-L. Chan, C.-D. Tsai, H.-H. Huang, D.-C. Chiou, and C.-P. Wu, "Photodetector with filter," *Electron. Lett.*, vol. 33, no. 2, pp. 163–164, Jan. 1997.
[7] O. Madelung, *Semiconductors—Basic Data*, 2nd ed. Berlin Heidelberg, Germany: Springer-Verlag, 1996, p. 151.
[8] CIE, Methods of Characterizing Illuminance Meters and Luminance Meters CIE Publication 69, 1987.